A QoS-enabled Holistic Optimization Framework for LTE-Advanced Heterogeneous Networks

Rajarajan Sivaraj[†], Ioannis Broustis[*], N. K. Shankaranarayanan[*], Vaneet Aggarwal[‡⊕], Rittwik Jana[*], and Prasant Mohapatra[†]

[†]University of California, Davis, [*]AT&T Labs Research, [‡]Purdue University

{*rsivaraj, pmohapatra*}@*ucdavis.edu*, {*broustis, shankar, rjana*}@*research.att.com, vaneet@purdue.edu*

Abstract—**LTE-Advanced (LTE-A) macro-cell deployments are being enhanced with small cells, i.e., low-power base stations, to increase the network coverage and capacity. However, simultaneous co-channel transmissions from macro and small cells cause increased inter-cell interference and under-utilize the spectrum resources at the small cells. The following LTE-A design techniques are used to improve system performance in such deployments: (i) Carrier Aggregation (CA) to increase capacity by using additional carrier bandwidth; (ii) enhanced Inter-Cell Interference Coordination (eICIC), that includes (a) Cell Selection Biasing (CSB) to increase small cell spectrum utilization via cell range expansion; and (b) *blanking* data transmission on the macro cells for a certain duration of time to increase cell-edge user throughput. Our objective is to maximize the CSB of the small cell, subject to user QoS constraints and blanking support from the macro cell. Towards this end, we develop an analytical model that captures the inter-dependency between eICIC techniques. We observe that, not accounting for the complex inter-dependencies between these techniques leads to a degraded network performance. We propose a framework that *jointly* optimizes eICIC and the assignment of multiple component carriers in an LTE-A deployment for increasing spectrum utilization at the small cells with appropriate blanking support from the macro cells. Our simulation results show that our approach increases the small cell spectrum utilization and aggregate cell-edge throughput by as much as 200%.**

I. INTRODUCTION

Mobile broadband traffic has been exponentially increasing over the last decade. To meet this growing demand, LTE small cells are deployed as an underlay to the existing macro cell network. Small cells are cheaper, lower-power base stations (called *eNodeB* or *eNB*) that can be densely deployed to satisfy the high data demand while offloading traffic from macro cells. LTE-Advanced (LTE-A) small cells typically share the same carrier frequency with nearby macro cells; as a result, their deployment can lead to high co-channel interference if resource sharing is not carefully planned [2]. The collective deployment of macro and small cells transmitting simultaneously on the same frequency channels to their respective User Equipment (UE) clients, is referred to as Heterogeneous Networks (Het-Nets). Such deployments are expected to dominate the broadband market in providing next-generation services [1]. LTE-A introduces the following techniques for improving performance in HetNets:

• *Carrier Aggregation (CA):* A multi-carrier deployment is one where the eNB can aggregate up to 5 different Component Carriers (CC) [3]. A CC is a frequency sub-band for an eNB ranging in bandwidth from 1.4-20 MHz. The CCs may belong to either the same frequency bands (intra-band CA), or different frequency bands, (inter-band CA) [4]–[6]. A UE can be scheduled on more than one CC concurrently, based on its traffic subscription. However, if it subscribes to a finite-buffer traffic associated with a lower-bound QoS, it is usually scheduled on a single CC [6].

• *Enhanced Inter-cell Interference Coordination (eICIC):* The transmission power of the macro eNB is significantly higher than that of a small cell eNB. If UEs choose between the small or a macro cell based on the value of received signal strength, this will likely to lead to relatively few users associating with the small cell. Lower user association to small cells under-utilizes the small cell spectrum resources [7] and therefore reduces or eliminates any expected capacity gains. Moreover, users associated to the small cell face interference from the adjacent macro resulting in poorer SINR. These problems are mitigated by using a combination of a *Cell-Selection Bias (CSB)* value broadcast by the small cell to attract users to it and the macro cell(s) suppressing transmission for a fixed number of time-slots. The UE adds the CSB value (in dB) to the Reference Signal Received Power (RSRP) from the small cell to bias its decision to attach to the small cell instead of the macro. Offloading UEs to the small cell thereby reduces the load on the macro. The geographic region comprising UEs attracted to the small cell using CSB is called the Cell-Range Expansion (CRE) region. The UEs in the CRE region are around the edges of the small cell, so they are vulnerable to any interference from the adjacent cells. eICIC addresses this issue by suppressing (or blanking) the macro cell's transmission of data on the interfering channels for a pre-determined number of time slots in the form of sub-frames [3] per downlink LTE frame, called *Almost Blank Subframes* (ABS) [2]. This blanking duration is called ABS length and is optimized to meet the QoS requirements of the UEs attached to the macro cell.

The need for joint optimization: Previous efforts have focused on improving the individual operations of CA and eICIC [2], [5], [8], [10]. However, our study explores them *jointly* and captures the intricate dependencies among these LTE-A techniques. For example, since inter-band CA enables the small-cell to transmit on multiple CCs, there could be different CRE regions, corresponding to each CC. As these CCs belong to different non-adjacent central band frequencies, they yield different radio channel conditions (such as path

---

loss) to their UEs. These channel dynamics, along with the instantaneous traffic load on each CC, affect the assignment of CCs to UEs and thereby their QoS. Accordingly, the channel- and traffic-aware CC assignment needs to use distinct CSB values across CCs. Hence, the corresponding CRE regions across CCs need not be identical and each CC may serve a different number of cell-edge UEs. This subsequently requires the macro to support different ABS lengths on different CCs based on the varying QoS requirements of the UEs across the distinct CRE regions. This suggests that *the application of one technique may impede the performance of another, unless applied carefully*.

Contributions: In this paper, we design a holistic optimization framework for LTE-A HetNets, which is the first of its kind to jointly account for the inherent design features of eICIC and CA. Moreover, we develop an analytical model for our framework. Specifically, our analysis is channel-aware and reveals the shape, properties, and UE population of the CRE region, accounting for traditional macro cell deployments such as Fractional Frequency Reuse (FFR) and Single Frequency Network (SFN). We show that optimally configuring the per-CC eICIC parameters (CSB and ABS), subject to QoS guarantees and blanking support from the macro on the corresponding CC, is *NP-Hard*. Based on our model, we propose a binary search-based iterative procedure to determine: (i) the assignment of CCs to UEs attached to the small and the macro cells, and (ii) the near-optimal CSB for each CC in the small cell along with the appropriate ABS length in the macro. We have developed new modules for eICIC and CA in the NS-3/LENA simulator [9] and implemented the CA, CSB and ABS functionalities. Based on our validated analytical configurations, we perform an extensive set of NS3 simulations to evaluate our joint optimization framework across different topologies and traffic conditions, using realistic network parameters and traffic subscriptions. Our simulations demonstrate that our framework improves the effective small cell spectrum utilization and the net CRE throughput by up to *200%*.

II. SYSTEM MODEL PRELIMINARIES

Our system model considers an LTE-A HetNet deployment, where each small cell is deployed within the coverage range of one or more interfering macro cells, as shown in Fig. 1, and uses significantly less transmission power. All small and macro cell eNBs use omni-directional antennae. We consider inter-band CA; Fig. 1 shows CA with 2 CCs. We consider a uniform distribution of UEs across the topology with a predefined Poisson density λ. The UEs subscribe to finite-buffer traffic applications which associate each subscription with a QoS requirement in terms of the required bit-rate. Our system model considers a $\log$-distance path loss model between any eNB-UE pair. The subscribed net user load is shared across all K CCs on any eNB and each attached UE is assigned to a single distinct CC on that eNB. The PRBs from that CC are scheduled using a proportional-fair scheduler to serve the UE for its QoS requirements. Application of CSB is considered on each CC deployed on the small cells only, for every LTE frame
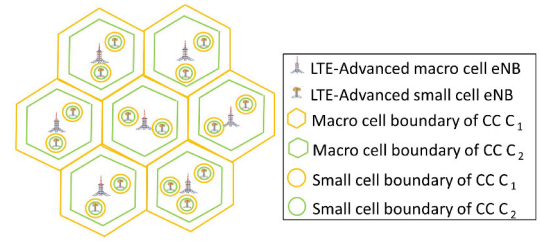
Fig. 1.   Illustrative System Model
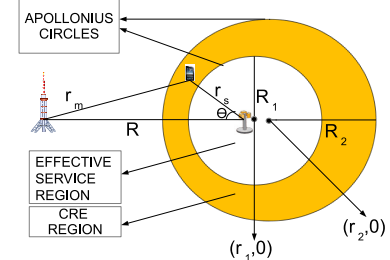
Fig. 2.   CRE region illustration

(lasting for 10 ms). Macro blanking with ABS is managed for the same CC on the interfering macro cells for that frame [2]. We assume that the overall UE population and affiliated traffic managed by each eNB remain static for a given LTE frame (or on the order of a few LTE frames).

III. ANALYTICAL MODELING AND ILLUSTRATIONS

In this section, we model the CRE region as a function of its CSB. We consider small cell topologies with (i) a single interfering single-carrier macro and (ii) multiple interfering single-carrier macros.

A. Single macro-cell interferer for FFR

Consider a macro cell m, a small cell s, and any UE indexed u belonging to a set of UEs $\mathbb{U}$ at any point in coordinate space. We assume that the macro cell is located at the origin $(0,0)$ and the small cell is located at $(R,0)$, as shown in Fig. 2. Let $r_{s,u}$ and $r_{m,u}$ denote the distances from the UE u to s and to m respectively. Let $\mathrm{rsrp}_s(u)$ be the Reference Signal Received Power (RSRP) value in linear scale at UE u with respect to s:

$$\mathrm{rsrp}_s(u) \triangleq \frac{P_s.\gamma.e^{-|h_{s,u}|}}{r_{s,u}^{\rho_s}} \tag{1}$$

where $P_s = P_s^{[T]}/f_c^{\alpha_s}$ is the power transmitted from s along the frequency band f_c of the CC $C_c \in \mathbb{C}$, $P_s^{[T]}$ is the transmission power at the small cell antenna, α_s is the frequency-dependent path loss exponent for s, and γ is the fraction of the transmission power available for the Cell-specific Reference Signal (CRS) [3], and $h_{s,u}$ indicates the shadow fading of the link between the small cell eNB s and the UE u. Usually, $h_{s,u}$ is a Gaussian variable; but here, since we assume that the eNB has a reasonable channel estimate/knowledge (as in Section II), $h_{s,u}$ is used as a deterministic value in Eqn. 1, and ρ_s is the distance-dependent path loss exponent. Similarly, the RSRP at UE indexed u w.r.t the fixed macro cell m, is given by:

$$\mathrm{rsrp}_m(u) \triangleq \frac{P_m.\gamma.e^{-|h_{m,u}|}}{r_{m,u}^{\rho_m}} \tag{2}$$

where $P_m = P_m^{[T]}/f_c^{\alpha_m}$ is the transmission power of the macro cell over CC C_c, and $h_{m,u}$ is the shadow fading between the macro-cell eNB m and UE u. We assume equal path loss exponents for the macro and small cells, i.e., $\rho_s = \rho_m = \rho$. If a CSB value $cb_{s,c}$ (in linear scale) is associated with small cell s on CC C_c and if the UE indexed u is inside the CRE region, the following conditions are satisfied:

(i) $rsrp_s(u) < rsrp_m(u)$, and (ii) $rsrp_s(u).cb_{s,c} \geq rsrp_m(u)$. Substituting with Eqn. (1) and (2), condition (i) becomes:

$$\frac{P_s.\gamma.e^{-|h_{s,u}|}}{r_{s,u}^\rho} < \frac{P_m.\gamma.e^{-|h_{m,u}|}}{r_{m,u}^\rho} \Rightarrow r_{s,u} > r_{m,u}.\left(\frac{e^{-|h_{s,u}|}}{e^{-|h_{m,u}|}}.\frac{P_s}{P_m}\right)^{\frac{1}{\rho}} \tag{3}$$

Similarly, condition (ii) is re-written as:

$$r_{s,u} \leq r_{m,u}.\left(\frac{e^{-|h_{s,u}|}}{e^{-|h_{m,u}|}}.\frac{P_s.cb_{s,c}}{P_m}\right)^{\frac{1}{\rho}} \text{ for } cb_{s,c} \geq 1. \tag{4}$$

Let $\mathbb{U}_{s,c}$ denote the set of UEs that satisfy both the conditions, given in Eqns. 3 and 4, corresponding to CC C_c. Let $u' = \arg \min_{u \in \mathbb{U}_{s,c}} (r_{s,u})$ and $u'' = \arg \max_{u \in \mathbb{U}_{s,c}} (r_{s,u})$. The boundaries of the CRE region are defined by the UEs in $\mathbb{U}_{s,c}$ at the minimum and maximum distances from s.

1) Defining the CRE region: Consider any point $\overline{u}$ in coordinate space. If θ is the angle of $\overline{u}$ from s with respect to the line-of-sight joining s and m, then we have:

$$r_{m,\overline{u}} = \sqrt{r_{s,\overline{u}}^2 + R^2 - 2r_{s,\overline{u}}R \cos\theta} \tag{5}$$

So, $r_{m,\overline{u}}$ is a constant multiple of $r_{s,\overline{u}}$. By the definition of *Apollonius circles* [12], the locus of points, whose ratio of distances from the two foci s and m is a constant, becomes a circle, as shown in Fig. 2. We define two such circles $\mathcal{C}_1$ and $\mathcal{C}_2$, whose circumferences contain the UEs u' and u'' respectively:

• $\mathcal{C}_1$ is the locus of points indicating the boundary of the coverage region of the small cell within which its signal (RSRP) is always greater than any interferer (termed as the small cell's effective service region, as defined in Sec. III-A2). $\mathcal{C}_1$ is given by the inner circle in Fig. 2 with center $(r_1, 0)$ and radius R_1.

• $\mathcal{C}_2$ is the locus of points indicating the boundary of the small cell's CRE region. $\mathcal{C}_2$ is the outer circle, as shown in Fig. 2, with center $(r_2, 0)$ and radius R_2. Here,

$$r_1 = \frac{R\left(\frac{P_m.e^{-|h_{m,u'}|}}{P_s.e^{-|h_{s,u'}|}}\right)^{\frac{2}{\rho}}}{\left(\frac{P_m.e^{-|h_{m,u'}|}}{P_s.e^{-|h_{s,u'}|}}\right)^{\frac{2}{\rho}} - 1}; r_2 = \frac{R\left(\frac{P_m.e^{-|h_{m,u''}|}}{P_s.cb_{s,c}.e^{-|h_{s,u''}|}}\right)^{\frac{2}{\rho}}}{\left(\frac{P_m.e^{-|h_{m,u''}|}}{P_s.cb_{s,c}.e^{-|h_{s,u''}|}}\right)^{\frac{2}{\rho}} - 1}, \tag{6}$$

and

$$R_1 = \frac{\left(\frac{P_m.e^{-|h_{m,u'}|}}{P_s.e^{-|h_{s,u'}|}}\right)^{\frac{1}{\rho}}R}{\left|\left(\frac{P_m.e^{-|h_{m,u'}|}}{P_s.e^{-|h_{s,u'}|}}\right)^{\frac{2}{\rho}} - 1\right|}; R_2 = \frac{\left(\frac{P_m.e^{-|h_{m,u''}|}}{P_s.cb_{s,c}.e^{-|h_{s,u''}|}}\right)^{\frac{1}{\rho}}R}{\left|\left(\frac{P_m.e^{-|h_{m,u''}|}}{P_s.cb_{s,c}.e^{-|h_{s,u''}|}}\right)^{\frac{2}{\rho}} - 1\right|}. \tag{7}$$

This result is quite valuable and non-obvious. Note that the two circles are not concentric and are not centered on the small cell. The region between the two circles is the CRE.

The circle centers have different offsets from the small cell location. If we consider the shadow fading as log-normal, unlike the deterministic model assumed in our framework, then these circles and the CRE region are not deterministic. This construct is customary in the field of radio coverage and these circles specify boundaries in a statistical sense. The CRE region is the intersection of the exterior of $\mathcal{C}_1$ and the interior of $\mathcal{C}_2$. Recall that the small cell is contained inside $\mathcal{C}_1$ and $\mathcal{C}_2$, which are non-concentric. $\mathcal{C}_1$ is completely contained in $\mathcal{C}_2$, because, for any polar coordinate ϕ, the boundary point distance for $\mathcal{C}_2$ is greater than that for $\mathcal{C}_1$, in brief. Note that in this case, we have $P_m.e^{-|h_{m,u''}|} > P_s.cb_{s,c}.e^{-|h_{s,u''}|}$. As $P_s/P_m \to 0$, this case occurs with probability going to 1. This further means that both $|r_1| > R_1$ and $|r_2| > R_2$, from Eqns. 6 and 7, are satisfied. So, the macro cell is outside both $\mathcal{C}_1$ and $\mathcal{C}_2$, in accordance to practical deployments. The area of the CRE region, $A_{s,c}$ corresponding to C_c of the small cell s, is then given by $A_{s,c} = \pi\left(R_2^2 - R_1^2\right)$. With u' and u'' as the CRE region boundaries, $A_{s,c}$ may also include UEs that are already attached to s without application of $cb_{s,c}$ due to the distinct shadow fading values $h_{s,u}$ and $h_{m,u}$ across UEs in $\mathbb{U}_{s,c}$.

2) Defining the Blocking Probability: We assume that users are distributed as a homogeneous Poisson Point Process with intensity λ. The area within a small cell where, with respect to any UE, the RSRP from the small cell is greater than that from any other cell is termed as the *effective service region*. We consider $\beta_{s,c}$ to be the total number of residual PRB pairs available in any CC C_c of the small cell eNB s. We refer to the case where there are more than $\beta_{s,c}$ UEs in the CRE region, corresponding to CC C_c, as *blocking*. If $\mathbb{P}(\mathfrak{B}_{s,c})$ denotes the *blocking* probability for C_c of s, given that $A_{s,c}$ is the area of the CRE region corresponding to C_c of s, then we have:

$$\mathbb{P}(\mathfrak{B}_{s,c}) = \mathbb{P}(N_{s,c} > \beta_{s,c} + \overline{n}_{s,c}) =$$

$$\sum_{n=\beta_{s,c}+1}^{\infty} \mathbb{P}(N_{s,c} = n + \overline{n}_{s,c}) = \sum_{n=\beta_{s,c}+1}^{\infty} \frac{(\lambda A_{s,c})^{(n+\overline{n}_{s,c})}.e^{-\lambda A_{s,c}}}{(n+\overline{n}_{s,c})!} \tag{8}$$

Here $N_{s,c}$ denotes the number of UEs in the CRE region corresponding to C_c of s, and $\overline{n}_{s,c}$ denotes the number of UEs that are already attached to C_c of s even without the application of the CSB value $cb_{s,c}$.

B. Multiple macro-cell Interferers for SFN

We now extend our model to consider scenarios where more than one macro cells interfere with a small cell. When multiple macro cell eNBs are present, a UE will associate to either the small cell or the macro cell which yields the highest RSRP value. Each of these macro cells in isolation would create a distinct CRE region around the small cell; however, since we need to determine only one net CRE region around the small cell, we need to collectively account for the distinct CRE regions corresponding to each interfering macro cell. Referring to Eqns. 3 and 4, for a given angle of orientation θ with respect to the small cell, let $r_s(c, \theta, 1)$ and $r_s(c, \theta, 2)$ denote the distances from the center of any small cell eNB s such

R	$E(N_{s,c})$	$\overline{N}_{s,c}$	R(m1,m2)	$E(N_{s,c})$	$\overline{N}_{s,c}$
100 m	474.37	475.94	(500,1200)	226.36	228.15
200 m	385.67	386.21	(600,1100)	132.24	134.84
300 m	266.86	270.31	(700,1000)	18.12	20.63
400 m	171.51	174.68	(800,900)	4.324	5.667
500 m	32.12	38.08	(900,800)	5.667	4.324

that: For any UE u whose distance from s along the direction θ, given by $\overline{r}_{s,u}(\theta)$, where $\overline{r}_{s,u}(\theta) \leq r_s(c,\theta,1)$, the RSRP of u from s (by substituting $\overline{r}_{s,u}(\theta)$ in Eqn. 1) is always greater than that from any highest interfering macro cell eNB $m_{u,\theta}$ alongside any UE location, given by the tuple (u,θ). However, for any u where $r_s(c,\theta,1) \leq \overline{r}_{s,u}(\theta) \leq r_s(c,\theta,2)$, (i) the RSRP of u from s as a result of CC C_c is always less than that from $m_{u,\theta}$, but (ii) with the addition of cb$_{s,c}$, the RSRP of u from s as a result of CC C_c is always greater than that from $m_{u,\theta}$. Hence, the UE u is in the CRE region along θ if and only if $r_s(c,\theta,1) \leq \overline{r}_{s,u}(\theta) \leq r_s(c,\theta,2)$. Here, the area of the CRE region corresponding to C_c of s corresponding to CSB cb$_{s,c}$ is:

$$A_{s,c} = \int_{\theta=0}^{2\pi} \int_{r_s(c,\theta,1)}^{r_s(c,\theta,2)} r \, \mathrm{d}r \, \mathrm{d}\theta \qquad (9)$$

Here, $r = \overline{r}_{s,u}(\theta)$, for any value of (u,θ). Now, the blocking probability $\mathbb{P}(\mathfrak{B}_{s,c})$, based on $A_{s,c}$, is as shown in Eqn. 8.

Inter small-cell interference: In the case of interference from other small cells in $\mathbb{S}$ on any UE r associated to the small cell s, r lies in the CRE region if:

$$\mathrm{rsrp}_s(r) - \sum_{s' \in \mathbb{S}} \mathrm{rsrp}_{s'}(r) < \sum_{m \in \mathbb{M}} \mathrm{rsrp}_m(r), \text{ and}$$
$$(\mathrm{rsrp}_s(r) - \sum_{s' \in \mathbb{S}} \mathrm{rsrp}_{s'}(r)).\mathrm{cb}_{s,c} \geq \sum_{m \in \mathbb{M}} \mathrm{rsrp}_m(r).$$

Here, $s' \in \mathbb{S}$ is any interfering small cell. If the first condition alone is false, then the UE is present in the effective service region of the small cell s. If the second condition alone is false, then the UE is associated to the macro cell m. Given this, it is generally recommended to sufficiently separate small cells from each other, during deployment, so as to limit the inter-cell interference among them.

A Monte-Carlo evaluation of our analytical model and our NS3 simulations (with the setup outlined in Section VI) shows around 95% accuracy in terms of the number of UEs in the CRE region ($E(N_{s,c})$ and $\overline{N}_{s,c}$, respectively), as shown in Table I. We use 500 users in and around the small cell, for a larger-scale stress testing. We run 50 independent NS3 trials with uniformly-distributed users around a small cell. R refers to the distance between the macro and the small cell eNBs for an FFR topology and $R(m1,m2)$ is the distance of the small cell eNB from 2 interfering macro cell eNBs at line-of-sight $m1$ and $m2$, respectively, in an SFN topology.

IV. FORMULATION AND HARDNESS

In this section, we discuss our insights on performance trade-offs, formulate the eICIC problem that accounts for CA, and discuss relevant NP-hardness.

Insights on performance trade-offs: The challenges in achieving the objective even for the simple case of a single small cell and a single interfering macro cell are:

1. A higher UE association to the small cell due to a large CSB value that increases the CRE region requires a larger ABS length from the interfering macros to satisfy QoS of the UEs in the CRE region. Such blanking might affect the QoS of UEs attached to the interfering macros. Use of larger ABS length becomes difficult if macros have a higher traffic load.

2. If UEs move from the macro to the small cell, the macro's load reduces. This might leave room for a higher ABS length. The trade-off between the two factors is not linear due to the non-linear signal characteristics, as discussed in Eqns. 1 and 2.

3. A lower UE association to the small cell requires a lower ABS length, but causes higher user load on the macros.

4. When including CA into the picture, new complications arise. The CSB values used across CCs on a small cell are different, resulting in non-identical CRE regions. This results in varying user association and traffic load on each CC. The small cell requests different ABS lengths for different CCs. When there is resource exhaustion on one of the CCs, the small cell has to decide between: (i) deflection of UEs to other CCs in the small cell, or (ii) deflection of the UEs to suitable CCs in the macro.

Optimization objective and Motivation: Our goal is to improve the effective spectrum utilization of the LTE-A small cells supporting CA for an efficient reuse of the deployed spectrum. Effective spectrum utilization is a measure of the fraction of the total frequency-time PRBs, scheduled to the UEs with the best-supported MCS values. Leveraging the lower deployment cost of small cells, our framework achieves this objective by offloading a large portion of the user-subscribed traffic load in the network to the small cells. Subsequently, it also reduces the traffic load on the macro cells, enabling them to accept more incoming UE connections and serve them for QoS. Our design accounts for addressing the above-discussed performance trade-offs between eICIC configuration parameters and the synergy between eICIC and CA. Towards this end, we aim to *maximize* the per-CC CSB of each small cell eNB s *jointly* with other CCs aggregated in s and further, *jointly* with other small cell eNBs in $\mathbb{S}$. This objective function is subject to support from the adjacent macro cells for the requested ABS blanking lengths on the corresponding CCs. A macro cell supports the requested ABS length on a CC, if and only if there is enough room for blanking, after the macro cell serves the UEs attached to it and associated to the CC for QoS. With a high broadcast CSB, our objective ensures higher spectrum utilization at the small cells and traffic offload from the macro.

Mathematical Formulation: As discussed above, our objective is to maximize the CSB of each CC aggregated in every small cell in a *joint* manner with other CCs and small cells, subject to (i) support from the adjacent macro cell(s) for the requested ABS length on the corresponding CC and (ii) QoS guarantees for the UEs served by any eNB. The mathematical formulation is written below:

$$\text{Maximize} \quad \mathrm{cb}_{s,c}; \; \forall C_c \in \mathbb{C}, \; \forall s \in \mathbb{S} \qquad (10)$$

$$\text{subject to} \quad 1 \le \text{cb}_{s,c} \le \text{CB}_{\text{Th}}$$

$$\omega_{s,c} \le \Omega_{m,c}; \ \forall m \in \mathbb{M}$$

$$\sum_{c=1}^{K} F_{s,c,u}.X_{s,c,u} \ge \tau_u; \ \forall u \in \mathbb{U}_s, \ \mathbb{U}_s \subseteq \mathbb{U}$$

$$\sum_{c=1}^{K} F_{m,c,\overline{u}}.Y_{m,c,\overline{u}} \ge \tau_{\overline{u}}; \ \forall \overline{u} \in \overline{\mathbb{U}}_m, \ \overline{\mathbb{U}}_m \subseteq \mathbb{U}$$

$$\sum_{c=1}^{K} X_{s,c,u} \le 1, \ \forall u \in \mathbb{U}_s; \ X_{s,c,u} = \{0,1\}$$

$$\sum_{c=1}^{K} Y_{m,c,\overline{u}} \le 1, \ \forall \overline{u} \in \overline{\mathbb{U}}_m; \ Y_{m,c,\overline{u}} = \{0,1\}$$

$$\bigcap_{s \in \mathbb{S}} \mathbb{U}_s \bigcap_{m \in \mathbb{M}} \overline{\mathbb{U}}_m = \{\emptyset\}$$

Input: We consider a given set of small cells $\mathbb{S}$, macro cells $\mathbb{M}$, aggregated set of CCs $\mathbb{C}$ on each eNB and a uniformly-distributed set of UEs $\mathbb{U}$. Each UE $u \in \mathbb{U}$ has a finite-buffer lower-bound bit-rate requirement for its subscribed traffic given by τ_u. A Proportional-Fair (PF) scheduler is used on each CC of any cell to allocate its PRBs to serve the assigned UEs on the CC for QoS. The scheduler yields a bit-rate of $F_{s,c,u}$ for any UE u served by CC C_c on a small cell $s \in \mathbb{S}$ and $F_{c,m,\overline{u}}$ for any UE $\overline{u}$ served by C_c on any macro cell $m \in \mathbb{M}$. $F_{s,c,u}$ is a function of the SINR *without interference from any of the macros* during ABS. The CSB $\text{cb}_{s,c}$ does not directly impact the rate $F_{s,c,u}$, as said in Section II (artificial broadcast).
Output: The output variables include (i) the choice of CSB $\text{cb}_{s,c}$ to be used on any CC C_c of any small cell $s \in \mathbb{S}$, (ii-A) the decision variable $X_{s,c,u}$ which yields 1 if the UE u is assigned to C_c of any s, or 0, otherwise, (ii-B) the decision variable $Y_{m,c,\overline{u}}$ if the UE $\overline{u}$ is assigned to C_c of any macro $m \in \mathbb{M}$, or 0, otherwise. This subsequently yields the set of UEs associated to any $s \in \mathbb{S}$ and $m \in \mathbb{M}$ given by $\mathbb{U}_s$ (that includes $N_{s,c}$ UEs, $\forall C_c \in \mathbb{C}$) and $\overline{\mathbb{U}}_m$ respectively, (iii-A) the ABS length requested on C_c by s given by $\omega_{s,c}$ and (iii-B) the ABS length granted on C_c by m given by $\Omega_{m,c}$.
Constraints: (i) The first constraint indicates that the choice of CSB on any CC of a small cell is limited by an upper-bound CSB threshold given by CB_{Th}. (ii) The second constraint indicates that the requested ABS length by any C_c of any $s \in \mathbb{S}$ is satisfied by the ABS length granted on C_c of the interfering macro cells $m \in \mathbb{M}$. (iii) The third and fourth constraints indicate that the rate achieved by any UE using our CC assignment, eICIC mechanism and the given PF scheduler meets the lower-bound threshold. (iv) The fifth and sixth constraints enforce that any UE is assigned onto at most one distinct CC deployed on any eNB. (v) The last constraint enforces exclusive cell association of the UEs among the cells.
Complexity: For the above problem, considering even the simple case of 2 CCs for a single small cell with an interfering macro makes the problem hard. This is typically shown by reducing the decision version of the NP-Complete Knapsack problem [14], where the given set of items are packed into bins in order to optimize a certain utility such as maximizing the net values of items subject to weight constraints of the bins,

to our simple case. We omit the details of the reduction proof for space constraints.

V. JOINT OPTIMIZATION PROCEDURE

Incorporating Carrier Aggregation: Consider the deployment of K CCs in the aggregated carrier $\mathbb{C}$ of a small cell. Assuming the same frequency-dependent path loss exponents α_s across all CCs (as in Section III A), the areas of the effective small cell service region and the CRE become independent of the central band frequencies, as $\frac{P_s}{P_m}$ (where m is any interfering macro) from eq. (3) becomes independent of f_c. Hence, the small cell effective service region is common for all CCs in $\mathbb{C}$. However, the areas of the CRE regions are dependent on the CSB values of the corresponding CCs, which are in turn dependent on the subscribed user load, residual PRBs and channel conditions on the respective CCs. In the presence of at most K distinct CSB values, there would be a maximum of K non-overlapping CRE regions, corresponding to the K CCs. With the same transmission power across all CCs, the cells corresponding to CCs operating on higher central band frequencies cause higher path loss values and hence, lower SINR values to the UEs scheduled on them. For an effective CA [4], [11], we consider a *non pre-emptive CC assignment* strategy that allocates PRBs from lower frequency CCs to the UEs present farther away from the eNB around its cell-edges, and those from higher frequency CCs to the ones present closer to the eNB. This maps the outer-CRE regions to lower-frequency CCs and inner-CRE regions to higher-frequency CCs. Our framework thus associates the CRE regions ranging from the inner-most to the outer-most with CCs in the order ranging from CC C_K, operating on the highest central band frequency f_K, to CC C_1, operating on the lowest frequency band f_1. The contours/boundaries of the CRE regions are given by: $r_s(c,\theta,1) = r_s(c+1,\theta,2)$, where $c \le K - 1$. Here, $r_s(c,\theta,1)$ is the lower-limit of the CRE region, corresponding to CC C_c, across direction θ and $r_s(c+1,\theta,2)$ is the upper-limit of the CRE region, corresponding to CC C_{c+1}. The CRE region corresponding to C_K is the inner-most, whose contours are defined by the lower and upper limits of the *net CRE region* along the direction θ, given by $r_s(K,\theta,1)$ and $r_s(K,\theta,2)$, where $c = K$ as described for Eqn. 9.

Given the non-preemptive multi-carrier resource allocation, we observe that a UE present in the CRE region corresponding to C_c can also be scheduled in PRBs of any CC $C_{c'}$ upon availability of sufficient residual bandwidth, if $c' < c$. In addition, a UE present in the CRE region, corresponding to C_c, **cannot** be scheduled in PRBs of any CC $C_{c'}$, if $c' > c$.

Blocking on any cell c in the case of CA happens when: **(i)** the number of UEs in the CRE region for C_c, given by $N_{s,c}$, exceeds $\beta_{s,c}$; and **(ii)** the number of UEs in the CRE region for C_c that exceed $\beta_{s,c}$ also exceed $\sum_{\forall c'} (\beta_{s,c'} - N_{s,c'})$, such that $c' < c$ and CC $C_{c'} \in \mathbb{C}$. Now, this last condition indicates a state of blocking in each cell c', which corresponds to CC $C_{c'}$, where $c' < c$, in accordance to our aforementioned first observation. Otherwise, the UE would have been admitted for service by

$C_{c'}$. Thus, the blocking probability of any CC C_c of s is:

$$\mathbb{P}(\mathfrak{B}_{s,c}) = \mathbb{P}(N_{s,c} > \beta_{s,c}, N_{s,c-1} + N_{s,c} - \beta_{s,c} > \beta_{s,c-1}, \dots$$
$$\sum_{c'=1}^{c} N_{s,c'} - \sum_{c''=2}^{c} \beta_{s,c''} > \beta_{s,1}) . \tag{11}$$

If $\overline{\mathfrak{B}}_{s,c}$ denotes the event that there is no blocking in the CRE region corresponding to CC C_c, then: $\mathbb{P}(\overline{\mathfrak{B}}_{s,c}) = \mathbb{P}(N_{s,c} \leq \beta_{s,c})$. We define that s is in a state of blocking if any one of the CCs is in the state of blocking. So, the net blocking probability of s, denoted by $\mathbb{P}(\mathfrak{B}_s)$, is given by:

$$\mathbb{P}(\mathfrak{B}_s) = \mathbb{P}(\mathfrak{B}_{s,K}) + \mathbb{P}(\overline{\mathfrak{B}}_{s,K} \bigcap \mathfrak{B}_{s,K-1}) + \dots$$
$$+ \mathbb{P}\left(\bigcap_{c=2}^{K} \overline{\mathfrak{B}}_{s,c} \bigcap \mathfrak{B}_{s,1}\right) \tag{12}$$
$$= \sum_{c=1}^{K} \mathbb{P}\left(\bigcap_{c'} \mathfrak{B}_{s,c'} \bigcap_{c''=c'+1}^{K} \overline{\mathfrak{B}}_{s,c''}\right) .$$

Now, for any C_c and C_{c-1}, $\mathbb{P}(\mathfrak{B}_{s,c}) \bigcap \mathbb{P}(\overline{\mathfrak{B}}_{s,c} \bigcap \mathfrak{B}_{s,c-1}) = 0$, as the events $\mathfrak{B}_{s,c}$ and $\overline{\mathfrak{B}}_{s,c}$ are mutually-exclusive. If there are N UEs associated to the small-cell across $\mathbb{C}$ as a result of non pre-emptive CA, then the total time complexity is $O(N^2)$.

Optimizing CSB and ABS: Next, we use our analytical model to optimize the feasible CSB values across CCs in order to maximize the objective function.

Initial Computation of CSB: To find the optimal CSB value across CCs meeting the ABS constraints using a binary-search method, we need to determine the lower and upper bounds for the CSB values. Recall from Section III that the criterion for association requires each attached UE from the CRE region to be allocated at least one PRB pair from the corresponding CC, such that its blocking probability is 0. Hence, the upper-bound CSB of C_c for any small cell s is that CSB value $cb^{\dagger}_{s,c}$ corresponding to which the net system blocking probability $\mathbb{P}(\mathfrak{B}_s)$ of s is 0. We obtain the upper-bound CSB $cb^{\dagger}_{s,c}$ of any C_c as follows. Let ψ_s be the vector of upper-bound CSB values for all K CCs aggregated on small cell s.

$$\psi_s = \max_{[cb_{s,1} \, cb_{s,2} \, \dots \, cb_{s,K}]}\{\arg \min_{[cb_{s,1} \, cb_{s,2} \, \dots \, cb_{s,K}]}\{\mathbb{P}(\mathfrak{B}_s)\}\}$$
$$cb^{\dagger}_{s,c} = \arg \max_{cb_{s,c}}(\psi_s) . \tag{13}$$

This is obtained by differentiating $\mathbb{P}(\mathfrak{B}_s)$ with respect to vector of CSB values across $\mathbb{C}$ and equating the derivative to 0.

$$\left[\frac{\partial \mathbb{P}(\mathfrak{B}_s)}{\partial cb_{s,1}} \, \frac{\partial \mathbb{P}(\mathfrak{B}_s)}{\partial cb_{s,2}} \, \dots \, \frac{\partial \mathbb{P}(\mathfrak{B}_s)}{\partial cb_{s,K}}\right] = 0 . \tag{14}$$

$cb^{\dagger}_{s,c}$ is the corresponding maximum among the minima and is the cth index of ψ_s obtained as a result.

Iterative Computation of CSB: Upon association to CC C_c of small cell s based on $cb^{\dagger}_{s,c}$, each of the UEs in the CRE region corresponding to C_c are allocated one PRB pair. Following their association, each of them subscribes to traffic with specific bit-rate requirements for QoS. However, the QoS requirements of any user-subscribed traffic, along with its channel conditions, might require more than one PRB pair to be allocated to the UE. As a result, all $N_{s,c}$ UEs from the corresponding CRE region

may not be served for their QoS as the total number of required PRB pairs $\overline{\beta}_{s,c}$ to serve the CRE UEs obviously exceeds the residual PRB pairs $\beta_{s,c}$. So, $cb^{\dagger}_{s,c}$ is not the optimal CSB value. On the other hand, even if the QoS requirements for the CRE UEs are met by assigning only one PRB pair to each UE based on $cb^{\dagger}_{s,c}$, there is a possibility that the ABS length requested by s on C_c, $\omega_{s,c}$, may not be supported by any of the interfering macros in $\mathbb{M}$ (only one, in the case of FFR). Since the requested ABS length cannot be granted, again $cb^{\dagger}_{s,c}$ is not the optimal.

In either of the above cases, we then determine the optimal CSB $cb^{\star}_{s,c}$ through a binary-search iteration by setting the lower bound of the CSB value as 1 (or 0 in dB scale) and the upper bound as $cb^{\dagger}_{s,c}$. We find the CSB value in the mid-point between the upper and lower bounds. We check if the corresponding requested ABS length is supported by the interfering macros. If yes, we shift the range to the right by setting the lower bound to the mid-point CSB value computed in the previous step. Else, we shift the range to the left by setting the upper-bound to the mid-point CSB value. We repeat the above steps until the instantaneous upper bound and lower bound in the current iteration do not differ by more than an approximated factor ϵ. At this point, the iteration stops and the CSB value computed at that iteration is returned as the near-optimal CSB $cb^{\star}_{s,c}$ for small cell s on CC C_c. This binary search procedure is summarized from steps 7 to 15 in Alg. 1, before finally returning the optimal value $cb^{\star}_{s,c}$. If neither case is true, i.e. when the QoS requirements of all the CRE UEs attached to C_c of s as a result of $cb^{\dagger}_{s,c}$ are satisfied, then $cb^{\dagger}_{s,c}$ is the optimal CSB value. For SFNs, the $\Omega_{m,c}$ is limited by that macro which can support the least ABS length. The time complexity required for this iteration to reach the optimal point $cb^{\star}_{s,c}$ is $O\left(\epsilon \log_2 cb^{\star}_{s,c}\right)$. It is to be noted that upon reducing the CSB value for any CC C_c at an iteration, we are reducing the number of CRE UEs $N_{s,c}$ corresponding to C_c thereby contracting the region. Consequently, the CRE region corresponding to C_{c-1} expands thereby accommodating more UEs that are deflected from C_c. Whereas, upon increasing the CSB value, the CRE region corresponding to C_c now encroaches upon the region served by C_{c-1} and contracts the region corresponding to C_c.

Co-existence of multiple small cells within common interfering macro set: Now, we consider a set of small cells $\mathbb{S}$ that interfere with a common set of macro eNBs $\mathbb{M}$. Here, each small cell $s \in \mathbb{S}$ may request for a different ABS length $\omega_{s,c}$ on CC C_c, when CSB is computed for each of them as in Alg. 1. Hence, a joint optimization strategy accounting for all the small cells in $\mathbb{S}$ is required to determine the near-optimal CSB values $\forall s \in \mathbb{S}$ that are supported by macro blanking. The joint optimization procedure is outlined in Alg. 2. Each small cell $s \in \mathbb{S}$ in some random order successively computes its near-optimal CSB value, $cb^{\star}_{s,c}$ on every CC C_c using Alg. 1. Now, since every small cell pulls over UEs from the macros, the number of UEs served by the macros keeps getting less and hence, the support for blanking keeps getting more, with successive iterations across $\mathbb{S}$. This is highlighted in lines 4 and 5 of Algorithm 2. This procedure is repeated until there

Algorithm 1 Optimal configuration of CSB $\text{cb}^\star_{s,c}$ $\left(\text{cb}^\dagger_{s,c}\right)$

1: Use the PF scheduler on C_c to determine $\overline{\beta}_{s,c}$ based on $\text{cb}^\dagger_{s,c}$. Compute $\omega_{s,c}$ and $\Omega_{m,c}$, $\forall m \in \mathbb{M}$
2: **if** $\overline{\beta}_{s,c} \leq \beta_{s,c}$ and $\omega_{s,c} \leq \min_{m \in \mathbb{M}} \Omega_{m,c}$, **then**
3:    Set $\text{cb}^\star_{s,c} := \text{cb}^\dagger_{s,c}$
4:    Return $\text{cb}^\star_{s,c}$
5: **else**
6:    Set $\text{cb}_{s,c}(l) = 1$, $\text{cb}_{s,c}(u) = \text{cb}^\dagger_{s,c}$ and $\text{cb}_{s,c} := \text{cb}_{s,c}(l)$
7:    **while** $\text{cb}_{s,c}(u) - \text{cb}_{s,c}(l) > \epsilon$ **do**
8:       Set $\text{cb}_{s,c} := \dfrac{\text{cb}_{s,c}(l) + \text{cb}_{s,c}(u)}{2}$.
9:       Use PF scheduler on C_c to determine $\overline{\beta}_{s,c}$ based on $\text{cb}_{s,c}$. Compute $\omega_{s,c}$ and $\Omega_{m,c}$, $\forall m \in \mathbb{M}$
10:       **if** $\overline{\beta}_{s,c} \leq \beta_{s,c}$ and $\omega_{s,c} \leq \min_{m \in \mathbb{M}} \Omega_{m,c}$, **then**
11:          Set $\text{cb}_{s,c}(l) := \text{cb}_{s,c}$.
12:       **else**
13:          Set $\text{cb}_{s,c}(u) := \text{cb}_{s,c}$.
14:       **end if**
15:    **end while**
16: **end if**
17: Set $\text{cb}^\star_{s,c} := \text{cb}_{s,c}$. Return $\text{cb}^\star_{s,c}$.

Algorithm 2 Joint Optimal configuration of CSB $(\mathbb{S}, \mathbb{M})$

1: Sort the small cells in any random round-robin order. Let $\mathbb{S}$ be the sorted set. Set $t := 1$
2: **while** $t == 1$ OR $\min_{m \in \mathbb{M}} (\Omega_{m,c}[t] - \Omega_{m,c}[t-1]) > \epsilon$, **do**
3:    **for all** $s \in \mathbb{S}$ **do**
4:       Call Algorithm 1 to determine $\text{cb}^\star_{s,c}$, $\forall C_c \in \mathbb{C}$
5:       Determine $\omega_{s,c}$. Update $\Omega_{m,c}[t] = \omega_{s,c}$, $\forall m \in \mathbb{M}$ and $\forall C_c \in \mathbb{C}$
6:       Set $\text{cb}_{s,c}(l) := \text{cb}^\star_{s,c}$ and $\text{cb}_{s,c}(u) := \text{cb}^\dagger_{s,c}$ as lower-bound and upper-bound CSB values, $\forall C_c \in \mathbb{C}$
7:    **end for**
8: **end while**
9: Set $\hat{\Omega}_c := \min_{m \in \mathbb{M}} \Omega_{m,c}[t]$ and return $\hat{\Omega}_c$, $\forall C_c \in \mathbb{C}$.

---

is no further support for blanking on any interfering macro in $\mathbb{M}$. During each iteration, the lower and upper-bounds of CSB are changed for each small cell. Since the support for macro-blanking (and hence, the CSB) keeps increasing with each iteration due to greater offload of traffic to the small cells, the lower bound of CSB for any C_c of a small cell s in the current iteration t is equal to the optimal CSB $\text{cb}^\star_{s,c}$ from the previous iteration $t-1$. This is indicated in step 6 and the loop runs from step 2 to step 8. The jointly-optimized ABS length is given by $\hat{\Omega}_c$ at the end of all iterations, as shown in step 9. If $\overline{\text{cb}}^\dagger_c = \max_{s \in \mathbb{S}} \text{cb}^\dagger_{s,c}$, then the loop in Alg. 2 has an upper bound time complexity of $O(\epsilon \log_2 \overline{\text{cb}}^\dagger_c)$. And for each small cell in $\mathbb{S}$, the time complexity has an upper bound of $O(\epsilon \log_2 \overline{\text{cb}}^\dagger_c)$. With the linear multiple of the total number of small cells in $\mathbb{S}$, the worst case time complexity is $O(\epsilon^2 \log_2^2 \overline{\text{cb}}^\dagger_c)$.

Performance Guarantees: Let N be the number of UEs associated to s as a result of our algorithm and $N^\star$ (*OPT*) be the maximum number of UEs as a result of an optimal CA and application of CSB. Let $c \leq K$ be an arbitrary CC index, used by our non-preemptive CA algorithm. We will analyze the

cases where the CC C_c contains a UE requiring more than $\frac{1}{2}B$ PRBs or not. If CC C_c serves a UE u with more than $\frac{1}{2}B$ PRBs, then the previous UEs in sorted order will all be allocated more than $\frac{1}{2}B$ PRBs and each CC with index $c' < c$ must contain any one of these. So, we have more than c UEs being allocated $\frac{1}{2}B$, so $N^\star \geq c$. Else if C_c does not serve a UE requiring more than $\frac{1}{2}B$ PRBs, then no CC indexed $c' > c$ contains a UE requiring more than $\frac{1}{2}B$ PRBs. So, the $K - c$ CCs together allocate PRBs greater than $2(K - c)$ UEs and none of these UEs can be scheduled on any CC $c' < c$. So, for any c, we have in all cases where either $N^\star \geq c$ or $N^\star \geq 2(K - c)$. Also, since N UEs are allocated as a result of our assignment, we know that $N^\star \geq N - c$. So, $N^\star \geq N - c \geq 2(K - c)$. So, we have $c \geq 2K - N$ Applying this to $N^\star \geq c$ and $N^\star \geq (N - c)$, we have $N \leq \frac{(N^\star + 2K)}{2}$, which indicates the approximation factor.

VI. PERFORMANCE EVALUATION

In this section, we evaluate the performance of our framework. We present our simulation setup followed by our results.

Simulation setup: We use the open source NS-3 simulator (LENA), which includes a complete implementation of uplink and downlink PHY and MAC layers. We extended the simulator by implementing the following additional LTE-A functionality: **(a)** ABS blanking for eICIC, **(b)** control interface between a small cell and macro cell during ABS, **(c)** implementation of CSB, **(d)** CA support using multiple network interfaces on an eNB, **(e)** Log-normal shadowing support and frequency-dependent path loss exponent for path loss computation in inter-band CA. We perform simulations for three cases: Scenario A with a single small cell and a single interfering macro; Scenario B with a single small cell with a single interfering macro; and Scenario C with many small cells and interfering macros. Scenarios B and C include CA. Each simulation result is based on an average of 50 instances of the various random variates (user placement, log-normal fading, traffic model). In Scenarios A and B, the number of traffic applications used by a UE follows a binomial distribution, i.e. there is a non-zero probability for any UE to subscribe for any number of traffic applications (incl. 0), up to a maximum subscription number. The choice of subscribing to any traffic application by any UE follows a uniform distribution. In Scenario C, we associate a uniform distribution to the number of non-zero UE-subscribed traffic applications, so that we test our mechanism using different traffic distributions. We consider a total of 320 users for Scenarios A and B, and a total of 600 UEs in Scenario C. The transmission powers of the small cells and the macro cell eNBs are 30 dBm and 47.78 dBm, respectively. We consider CA of CCs corresponding to central band frequencies of 748 MHz and 2125 MHz, each deployed over a 10 MHz bandwidth. The heights of the macro cell eNB, small cell and the UEs are considered to be 32m, 10m and 1.5m, respectively, equipped with omni-directional isotropic antenna. We assume a log-distance path loss model with a distance-dependent and frequency-dependent loss exponents of 3.52 and 2.16, respectively. The total number of UEs corresponding to scenarios A and B is 320, while it is 600 for scenario C.
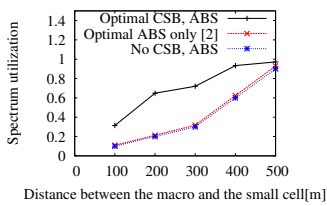
Fig. 3. Spectrum-utilization of the small cell (Scen. A)
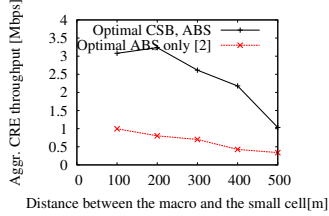
Fig. 4. Aggregate Achievable throughput of cell-edge users (Scen. A)
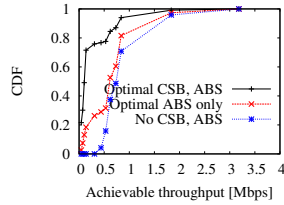
Fig. 5. CDF of the TBS supported by small cell UEs (Scen. A)
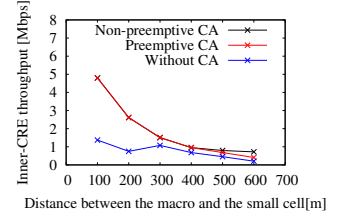
Fig. 6. Aggregate achievable throughput of inner-CRE UEs (Scen. B)

Fig. 7. Additional spectrum utilization in CRE of multi-carrier small cell (Scen. B)

Fig. 8. Spectrum utilization of multi-CC small cell with many interfering macros (Scen. C)

There is uniform distribution of users around the cell. The traffic subscription across UEs follows a binomial distribution with uniform probabilities for choosing traffic. We consider a proportional-fair scheduling algorithm.

In Scenario A with a single carrier small cell, the users in the effective service region subscribe to traffic applications with minimum-acceptable rates of 32 kbps, 128 kbps and 512 kbps, following a binomial distribution with a maximum of 2 traffic subscriptions per UE. The average binomially-distributed traffic in the rest of the single-carrier macro is around 6 Mbps. In Scenarios B and C the traffic subscription for the users in the effective small cell service region (considered with minimum-acceptable traffic rates of 64 kbps, 128 kbps and 768 kbps) is uniformly-distributed with one traffic subscription for every UE. Each of the remaining UEs subscribe to exactly one of the traffic applications with rates 32 kbps, 64 kbps and 128 kbps with uniform probabilities.

Scenario A Results: This scenario has small cells placed at varying distances from a single interfering macro without CA. Fig. 3 shows the small cell spectrum utilization versus distance between the small cell and the macro cell. The cell spectrum utilization is defined as the fraction of the frequency-time resources in the cell that are utilized, based on user association. Our proposed solution can be compared with the approach in [2] and the baseline case with no eICIC. As the distance increases, the small cell effective service region increases, bringing more UEs into the small cell, and thus increasing the small cell spectrum utilization. Our mechanism outperforms [2] in small cell spectrum utilization metric by an overall average of above 100%, with a minimum of 5% at R=500m and maximum of 201% at R=200m. At lower distances, since utilization is low, our proposed scheme tries to use a relatively large CSB to attract UEs to the small cell, which needs a relatively higher ABS length. Since the macro can only support a limited ABS length after serving its UEs, this tends to depress the spectrum utilization improvement. Fig. 4 shows the aggregate achievable downlink throughput of the cell-edge UEs in the CRE region attracted to the small cell, as a function of the distance between the small cell and the macro cell. This metric depends on the best-supported MCS levels of the UE. Upon comparison with [2], our mechanism improves the aggregate downlink achievable throughput of the small cell by an average of above 200%. This is achieved due to our focus on higher user association to the small cell, while satisfying their QoS.
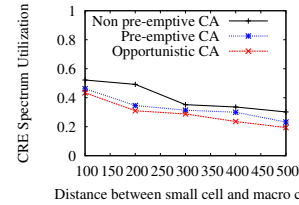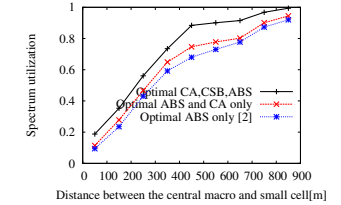
The number of CRE users, and thus the aggregate throughput, however decreases with distance as they are limited by the supported ABS length. Fig. 5 shows the Cumulative distribution

TABLE II
DECLINE IN SYSTEM PERFORMANCE DUE TO INEFFECTIVE USE OF CA

Throughput	PMF of throughput supported		
(kbps)	Non-preemp. CA Proposed	Pre-emp. CA	Non-preemp. CA Oppo.
44	5/17	3/12	0
72	2/17	2/12	0
103	1/17	2/12	0
139	5/17	4/12	0
306	4/17	1/12	0

function (CDF) of the per PRB achievable throughput of all the UEs, served by the small cell eNB. The plot indicates the fraction of UEs supporting any throughput value less than or equal to the corresponding throughput. Our proposed solution can be compared with the approach in [2] and the baseline case, i.e. no eICIC (no CSB, no ABS). Since [2] focuses on maximizing the achievable throughput of any individual UE by an appropriate cell association based on its SINR, it is reasonable that a larger fraction of UEs support higher throughput values in [2] than in ours. However, we achieve a higher aggregate small cell downlink throughput as discussed in previous results. Our approach fully exploits the investment in the small cell and provides the maximum offload of traffic from the macro. Our metric outperforms [2] in small cell UE association by 284%.

Scenario B Results: This scenario has small cells with CA at varying distances and a single interfering multi-carrier macro cell, both supporting CA. The inclusion of CA is a core feature of our work, and we explore *non pre-emptive* CA as well as *pre-emptive* CA. Our proposal uses *non pre-emptive* CA, as discussed in Sections II and III, while *pre-emptive* CA uses all

CCs simultaneously for allocation to the UEs in a round-robin manner. Fig. 7 shows the spectrum utilization, based on user association, as a function of the distance between the small cell and the macro cell for three cases. Our proposed solution that uses *non pre-emptive* CA is compared against: **(a)** a case where *non pre-emptive* CA is employed with a throughput-maximization strategy, where UEs closer to the small cell are first assigned to available resources in the lower-frequency CC, and **(b)** a *pre-emptive* CA technique. The actual number of users served by the higher frequency CC (2125 MHz) can be seen in Table II. With our proposed scheme, more users are attached to the small cell. The third column shows that the *non pre-emptive CA* with the maximum throughput strategy does not have any CRE users. This is because it schedules the UEs with higher SINR on lower-frequency CC (748 MHz) so as to improve the net system downlink throughput. So, the cell-edge UEs are scheduled on the higher-frequency CC. But due to the higher path loss yielded by the 2125 MHz CC, the corresponding CRE UEs, already impaired by farther distance, cannot be served for QoS. Thus, the PRBs of 2125 MHz CC are under-utilized. *This underscores our claim that it is important to optimize CSB, ABS, and CA jointly.* Our technique outperforms the non-preemptive opportunistic CA technique [11], [4] by 37% and pre-emptive CA by 22%, on average. It improves UE association to the higher frequency (2125 MHz) cell by 42%, overall, as seen in Table II. The total improvement in aggregate small-cell downlink throughput due to our scheme over pre-emptive CA is 77.5%. The improvements of up to 75% in the throughput of the inner-CRE region corresponding to 748 MHz, as a result of our framework, is shown in Fig. 6.

Scenario C Results: This scenario has small cells at varying distances and seven interfering macros, all supporting CA. Fig. 8 shows small cell spectrum utilization versus distance between the small cell and the central macro cell. Our proposed solution offers higher user association and effective spectrum utilization. We compare our approach with the technique in [2] evaluated over both pre-emptive CA and our proposed CA. Due to multiple interfering macro cells, the CRE region and hence the number of CRE UEs are smaller, compared to a single interfering macro cell. And due to pre-emptive CA, the larger path loss on the higher-frequency 2125 MHz CC causes a heavily under-utilized spectrum and cannot guarantee QoS. Hence, our technique outperforms the compared ones by at least 8% and 5% for R=850m to a maximum of 100% and 65% for R=100m, averaging 22% and 21% overall, over the scheme in [2] over pre-emptive and non pre-emptive CA.

VII. Related Work

Recent studies have assessed the efficiency of eICIC on network performance [10] and CA techniques [5], independently. The work most relevant to ours is [2]. The authors propose algorithms for optimizing user association to small/macro cell by maximizing the downlink channel quality, in the absence of CA. They determine an optimal ABS value based on user association and subsequently choose the CSB. Our work differs in the objective function where we maximize the per-CC CSB

of the small cell along with CA to increase its utilization and offload as much traffic as possible from the macro. The authors in [8] present a survey of frequency-domain and time-domain ICIC techniques for a HetNet supporting CA, along with transmission power adaptations across the constituent CCs. However, their work does not assess the inter-dependencies between these techniques. In [13], the authors address interference management issues for resource allocation in femto-cell deployments. As opposed to [13], we perform interference management in time-domain, while considering the same frequency deployment across cells. Due to the heterogeneous transmission capabilities between cells and a non-linear path loss model, sub-channel zoning does not result in fair splitting of dedicated PRBs between them for guaranteeing QoS.

VIII. Conclusion

We proposed a framework that exploits the inherent properties of LTE-A features towards efficiently planning HetNet deployments. Our analytical model captures the inter-dependency between CA and eICIC. Based on our model, we proposed an optimization framework to maximize the per-CC CSB subject to ABS and QoS constraints. Our simulations demonstrate significant performance benefits of above 200% for our proposed joint optimization approach over existing techniques in terms of the evaluated system utilities.

References

[1] 3GPP, "TR 36.814 Evolved Universal Terrestrial Radio Access (E-UTRA); Further Advancements for E-UTRA PHY Aspects; Rel. 9."

[2] S. Deb, P. Monogioudis, J. Miernik, and P. Seymour, "Algorithms for Enhanced Inter Cell Interference Coordination (eICIC) in LTE HetNets," *IEEE/ACM Trans. on Networking*, vol. 22, no. 1, Mar. 2013.

[3] S. Sesia, I. Toufik and M. Baker, "The UMTS Long Term Evolution, From Theory to Practice," *John Wiley and Sons Ltd; 2nd edition*, 2011.

[4] R.Sivaraj, A. Pande, K. Zeng, K. Govindan, and P. Mohapatra, "Edge-prioritized channel- and traffic-aware uplink carrier aggregation in LTE-advanced systems," in *IEEE WoWMoM*, 2012.

[5] G. Yuan et al. "Carrier aggregation for LTE-advanced mobile communication systems," *IEEE Comm. Mag.*, vol. 48, no. 02, Jan. 2010.

[6] K. I. Pedersen, F. Frederiksen, C. Rosa, H. Nguyen, L. G. U. Garcia and Y. Wang, "Carrier Aggregation for LTE-Advanced: Functionality and Performance Aspects," *IEEE Comm. Mag.*, vol. 49, no. 6, Jun. 2011.

[7] S. Vasudevan, R. N. Pupala and K. Sivanesan, "Dynamic eICIC - A Proactive strategy for improving spectral efficiencies of heterogeneous LTE cellular networks by leveraging user mobility and traffic dynamics," *IEEE Trans. Wireless Comm.*, vol. 12, no. 10, pp. 4956-4969, 2013.

[8] L. Lindbom et al. "Enhanced Inter-Cell Interference Coordination for Heterogeneous Networks in LTE-Advanced: A Survey," http://arxiv.org/abs/1112.1344.

[9] LTE-EPC Network Simulator (LENA), http://iptechwiki.cttc.es/.

[10] D. L.-Prez, I. Gven, G. de la Roche, M. Kountouris, T. Q. S. Quek, and J. Zhang, "Enhanced Inter-Cell Interference Coordination Challenges in Heterogeneous Network," CoRR, abs/1112.1597, 2011.

[11] R. Sivaraj, A. Pande, and P. Mohapatra, "Spectrum-Aware Radio Resource Management for Scalable Video Multicast in LTE-Advanced Systems," in *IFIP Networking*, 2013.

[12] E. Kasner and F. Supnick, "The Apollonian Packing of Circles," *Proc. National Academy of Sciences USA*, vol. 29, no. 11, pp. 378-384, 1943.

[13] M. Y. Arslan, J. Yoon, K. Sundaresan, S. V. Krishnamurthy and S. Bannerjee, "FERMI: A FEmtocell Resource Management System for Interference Mitigation in OFDMA Networks," *IEEE/ACM Transactions on Networking*, vol. 21, no. 05, Oct. 2013.

[14] H. Kellerer, U. Pferschy and D. Pisinger, "Knapsack Problems," in *Springer. doi:10.1007978-3-540-24777-7*, 2004.